Progress In Electromagnetics Research C, Vol. 62, 149–156, 2016

A Compact Multiband Omnidirectional GNSS Antenna for Artillery Projectile Applications

Weiwei Liu, Yufa Sun*, Dong Zhou, Shaoqi Hu, and Ming Yang

Abstract—A compact multiband omnidirectional antenna for the reception of GNSS signals on artillery projectiles is designed in this paper. The proposed antenna consists of a metallic cone comprising a T-shaped monopole. It exhibits a broad bandwidth from 1.22 GHz to 1.28 GHz and from 1.44 GHz to 1.75 GHz, covering GPS L1, Galileo E2-L1-E1, GLONASS G1 and G2, CNSS B1 and B3. Measured results show that an omnidirectional radiation pattern is achieved, and the non-circularity in the azimuthal plane (xy-plane) is less than 2 dB for all the desired bands. Then the measured 6 dB beamwidth is about 110° in the presence of a finite 20 millimeters (mm) radius ground plane. Such an antenna has the potential to be easily used for small artillery projectiles.

1. INTRODUCTION

The Global Navigation Satellite System (GNSS) is widely used for navigation and precise position measurement. A quad-band probe-fed annular patch antenna for GNSS application has been designed with the diameter of $0.365\lambda_0$ (λ_0 is the wavelength in free space) [1]. In the design, four patches are stacked to achieve multiband operation, and circular polarization is obtained by complex quadrature phase feeding network. A compact GPS antenna which consists of four inverted-F-type elements and a series feeding network has been proposed [2]. This antenna is a good candidate for signal reception on artillery projectiles over 1.57–1.62 GHz, but it only covers the single GPS L1 band. In [1] and [2], the peek direction of the radiation pattern is vertical to the antenna plane without the characteristic of omnidirectional radiation. While omnidirectional radiation plays a significant role in enhancing the stability of signal reception, especially in artillery projectile applications.

The projectile trajectory is accurately determined with GNSS and then used in guiding it more accurately to the target. During the flight, the aerial vehicle has been in high speed movement and rotation state. In order to receive stable navigation signals during the rotating process, omnidirectional radiation with good non-circularity characteristic in the plane normal to the aircraft is required.

Various types of GNSS antennas are capable of obtaining the omnidirectional radiation pattern. A new omnidirectional circularly polarized (CP) antenna with good performance has been proposed [3]. However, the antenna size is quite large with the diameter of around $0.5\lambda_0$. Moreover, this antenna could not be installed directly in the artillery fuze with metal ground. Another Omnidirectional dual-band dual circularly polarized microstrip antenna using TM_{01} and TM_{02} modes has been designed with the diameter of $0.33\lambda_0$ [4]. These antennas exhibit good circular polarization properties. However, heavy gauge is usually required to be implemented. Projectile antennas have strict requirements on installation space which looks like a cone. The limited volume for designing antennas has moved designers to linearly polarized antenna solutions for GNSS applications [5–8].

Printed dipole [9] and loop antennas are conventional omnidirectional antennas. Printed dipole antenna provides a triple-band operation with total volume of $0.477\lambda_0 \times 0.528\lambda_0 \times 0.063\lambda_0$ [10]. A

Received 12 January 2016, Accepted 25 February 2016, Scheduled 2 March 2016

* Corresponding author: Yufa Sun (yfsun_ahu@sina.com).

The authors are with the Key Lab of Intelligent Computing & Signal Processing, Ministry of Education, Anhui University, Hefei 230601, China.

horizontally polarized omnidirectional planar antenna which consists of four printed arc dipoles is developed with the diameter of $0.556\lambda_0$ [11]. A dual-band printed dipole antenna is designed by combining a rectangular and two L-shaped radiating elements [12]. A dual-meander folded loop antenna [13] is difficult to avoid the defect of huge assembling space and bad mechanical strength. The conical monopole is a well-known antenna with broad bandwidth and good radiation efficiency. Various work has been done to investigate this kind of antenna, such as the conventional conical monopole and biconical antenna. Conical monopoles with optimized structure have been proposed. In [14], the antenna consists of a monoconical conducting body and a parasitic ring shorted to a ground plate. The diameter of this antenna is $0.22\lambda_0$ and the ground plate is $0.93\lambda_0$. The shorted top hat monocone antenna [15] also has huge antenna size though it has the characteristic of omnidirectional radiation.

In this paper, a compact omnidirectional GNSS antenna with wide impedance bandwidth and good non-circularity characteristic is presented. A novel way of combining the conical antenna which is capable of achieving wide impedance bandwidth and the T-shaped monopole antenna miniaturizes the overall antenna size. The ground plane of this antenna has a diameter of 40 mm ($0.168\lambda_0$) and the total height of this antenna is around 47 mm ($0.199\lambda_0$). The proposed antenna covers the bands of GPS L1 (1.575 ± 0.012 GHz), Galileo E2-L1-E1 (1.559–1.591 GHz), GLONASS G1 (1.598–1.609 GHz), GLONASS G2 (1.242–1.251 GHz), Compass Navigation Satellite System (CNSS) B1 (1.558–1.563 GHz), and CNSS B3 (1.258–1.278 GHz) with omnidirectional radiation pattern. Since there is no dielectric substrate, the radiation efficiency is very close to ideal, which is beneficial for the antenna gain data. Further, both the conical antenna and the T-shaped monopole are mounted on the ultra small ground plane using single-fed structure. This kind of compact multiband GNSS antenna with omnidirectional radiation for artillery projectile applications has seldom been reported.

2. ANTENNA GEOMETRY

The structure of the designed antenna is shown in Fig. 1. This hybrid antenna consists of a conical radiator and a T-shaped monopole, both sharing a common feeding point and mounted on a FR4

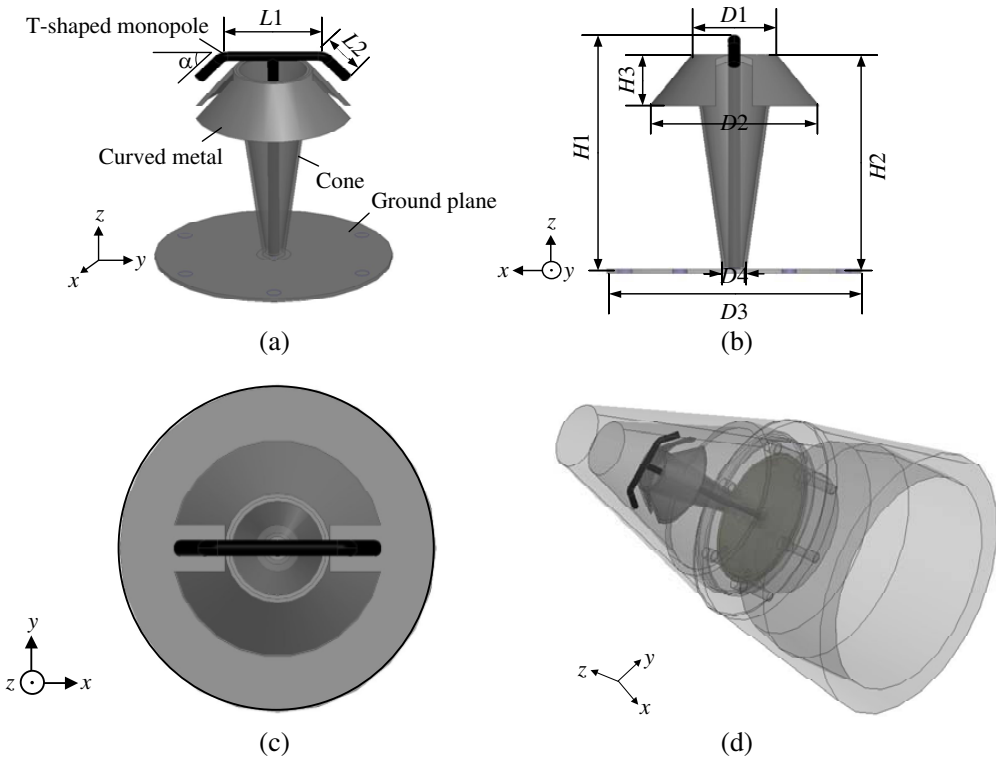

Figure 1. Structure of the designed antenna, (a) 3D view; (b) side view; (c) top view. (d) Proposed antenna installed inside an artillery fuze.

printed circuit board (PCB) using a double-sided copper-clad boards. And the feed region of the upper surface of the PCB is not clad with copper. The conical radiator is modified by merging a cone with two symmetric curved metals at the position referred to as the junction location in order to fully utilize the available space. A T-shaped monopole passes through the internal cavity of the cone and joints at the bottom of it. The bottom diameter of the cone is 5.0 mm ($D4$) and the top diameter of the cone is 14.0 mm ($D1$). Besides, the two arms of the T-shaped monopole are angled to 62 degrees referenced to the ground plane for further utilizing the available space. The total arm length of the T-shaped monopole is L ($L = L1 + 2 \times L2 = 28$ mm). The main-arm length of the T-shaped monopole ($H1$) is 46 mm ($0.194\lambda_0$). A conventional conical antenna is usually placed on a broad metallic ground plane or a large cone, requiring huge assembling space. The material of the whole antenna is metallic conductor, which is critical to the antenna gain.

The evolution of the proposed antenna is shown in Fig. 2(a), with the corresponding simulated reflection coefficient results presented in Fig. 2(b). The construction of the antenna begins with the conventional cone (antenna I) which resonates at around 1.77 GHz. Then two symmetric curved metals (antenna II) generate the electromagnetic coupling with the cone and the current path is longer, thus the resonance of the upper band moves to lower frequency and actually reduce the antenna size. As we all know, the measured resonance will shift compared with the simulated one more or less. Here the two slots are cut on the curved metal beneath the arm of the T-shaped monopole in order to facilitate the adjustment of resonance and not to exceed the installation space. When a T-shaped monopole is employed (proposed antenna), multiband antenna is achieved. From Fig. 3, the radiation patterns at 1.268 GHz for the three antennas have some difference, while radiation patterns at 1.575 GHz for the three antennas are almost the same. Because the reflection coefficient results of antenna I and II are not as good as the proposed antenna at 1.268 GHz, while all the three antennas have good reflection coefficient results at 1.575 GHz. From Fig. 2 and Fig. 3, we can conclude that the conical radiator is

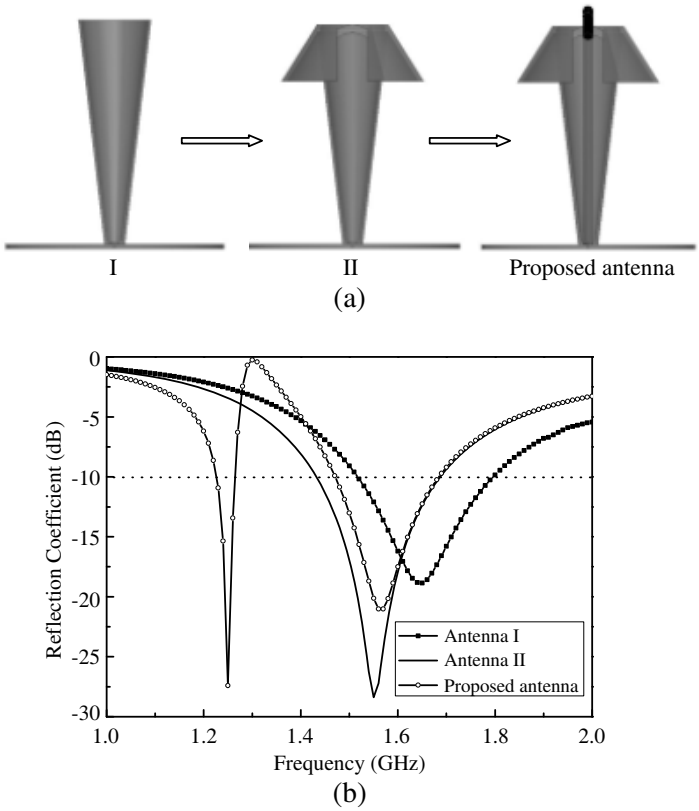

Figure 2. (a) Design evolution of the proposed antenna. (b) Corresponding simulated reflection coefficient results.

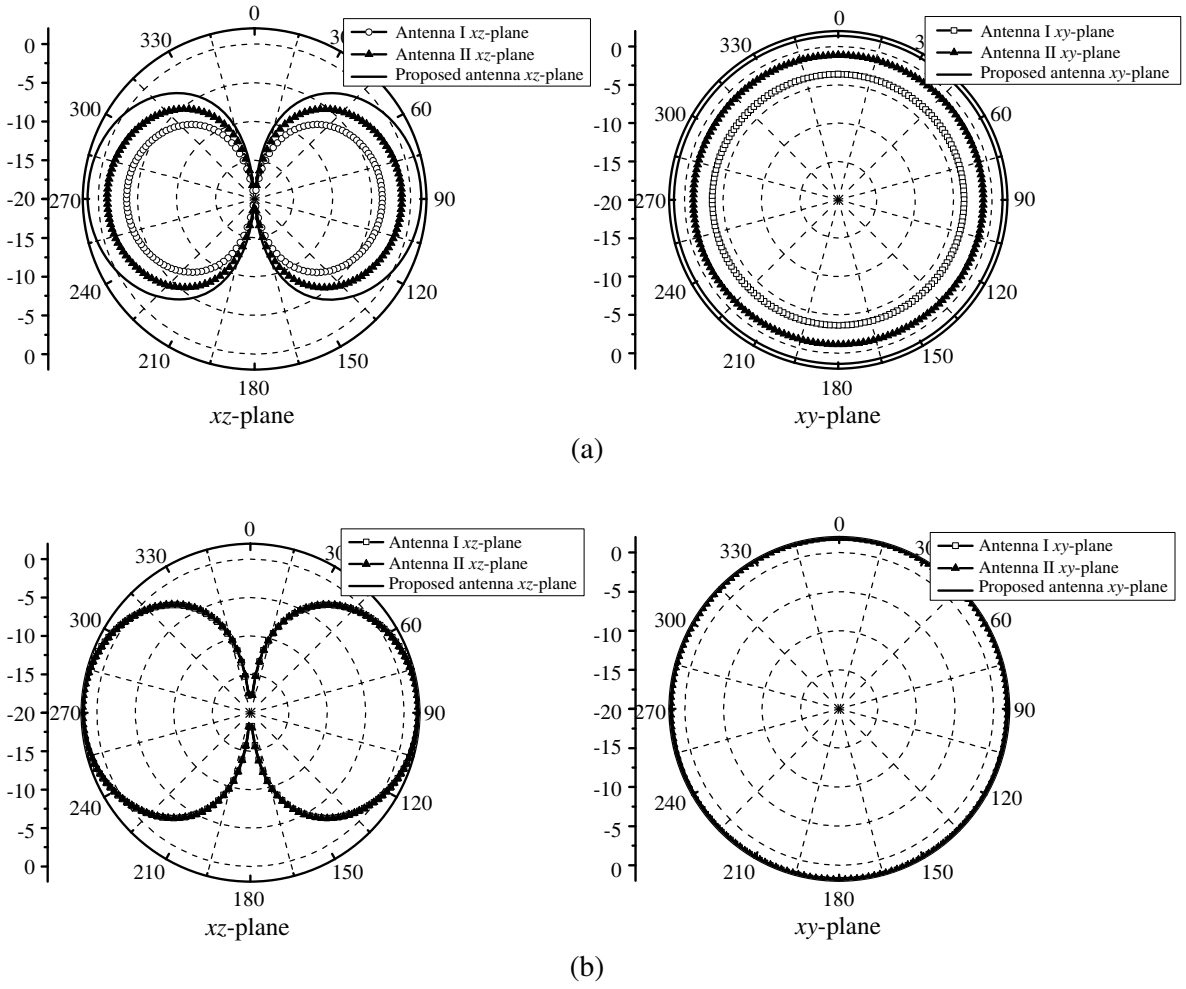

Figure 3. Simulated 2-D radiation patterns at (a) 1.268 GHz, (b) 1.575 GHz for antenna I, antenna II and proposed antenna (Unit: dBi).

designed to have a resonance at the upper bands (L1/B1), being the main radiation part of the whole antenna, while the T-shaped monopole is designed to have a resonance at the lower band (B3).

3. SIMULATION AND MEASUREMENTS

The simulation of the antenna design was carried out by Ansoft HFSS. Effects of some parameters on reflection coefficient of the designed antenna are analyzed. The reflection coefficient for three discrete values of α is depicted in Fig. 4. When the parameter α increases, the coupling between T-shaped monopole and curved metals is strengthened, hence, the lower resonant point moves to lower frequency. As the cone height $H2$ decreases, the two resonance points shown in Fig. 5 move to upper frequencies. From Fig. 5, it can be concluded that the height of cone is the major factor of the upper resonances (L1/B1). The effects of the height of H3 have also been studied. Similar results have been obtained, therefore they are not included here.

It can be observed from Fig. 6 that as the value of $D4$ is varied from 4.0 to 6.0 mm, the reflection coefficient will abruptly be changed. It illustrates that $D4$ plays an important role in impedance matching. Because it is well known that the input impedance response of a conical antenna is primarily determined by the feed region [17]. As we can see, when $D4$ is 5.0 mm, the performance of antenna is the optimum.

To validate the design strategy, a photograph of the actual multiband antenna was fabricated, as

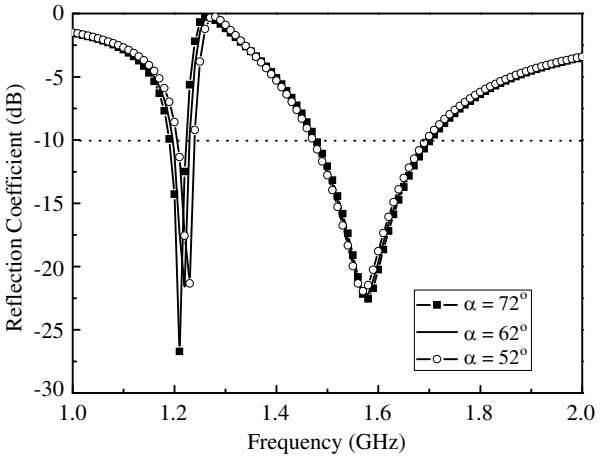

Figure 4. Reflection coefficient for three discrete values of α.

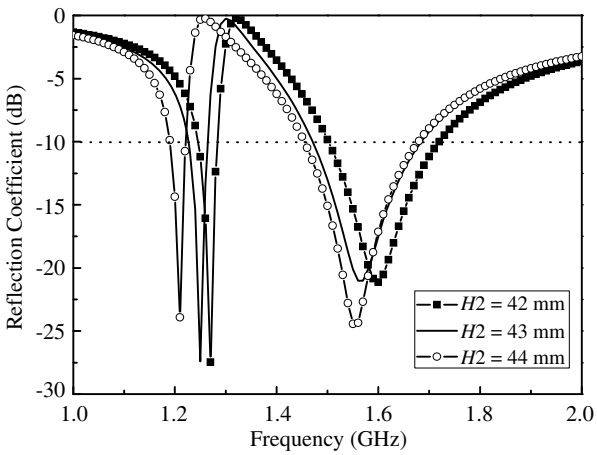

Figure 5. Reflection coefficient for three discrete values of $H2$.

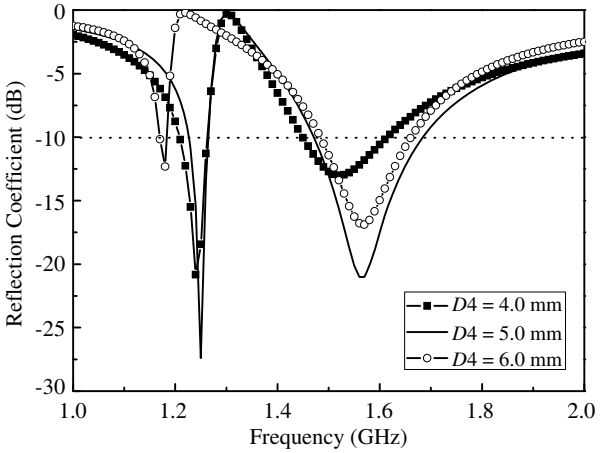

Figure 6. Reflection coefficient for three discrete values of $D4$.

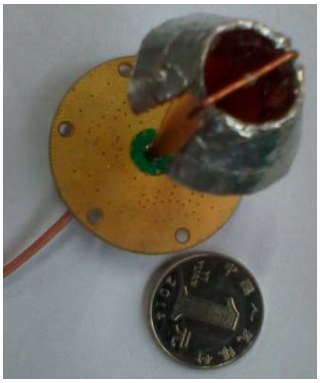

Figure 7. Photograph of actual fabricated prototype.

depicted in Fig. 7. The design parameters of the prototype are as follows: $L1 = 18\,\text{mm}$, $L2 = 5.0\,\text{mm}$, $\alpha = 62°$, $H1 = 46\,\text{mm}$, $H2 = 43\,\text{mm}$, $H3 = 16\,\text{mm}$, $D1 = 14\,\text{mm}$, $D2 = 28\,\text{mm}$, $D3 = 40\,\text{mm}$, $D4 = 5.0\,\text{mm}$. In this design, the reflection coefficient was measured by using an Agilent Technologies E5071C network analyzer. The measured reflection coefficient versus the frequency is shown in Fig. 8, which compares favorably with the simulated one. A slight discrepancy in the upper band is attributed to the effects of some mechanical inaccuracies and the cable line in the measurement. Measured results show that the designed antenna is feasible to cover the three desired resonant frequencies by means of combing the conical radiator and T-shaped monopole.

The 6 dB beamwidth and peak gain of the designed antenna corresponding to the frequencies are listed in Table 1.

From Table 1, it is noted that the peak gain increases with the resonance points moving to upper frequencies. Meanwhile, the measured results are generally lower than the simulated ones. Some discrepancies in the measured peak gain and beamwidth of the left and right sides are primarily attributed to some mechanical inaccuracies.

The measured and simulated radiation patterns of the proposed antenna are shown in Fig. 9, respectively, at the frequencies of 1.268, 1.561 and 1.575 GHz. The omnidirectional in the xy-plane and a '∞' shaped radiation pattern in the xz-plane are achieved in all desired bands. With reference to the

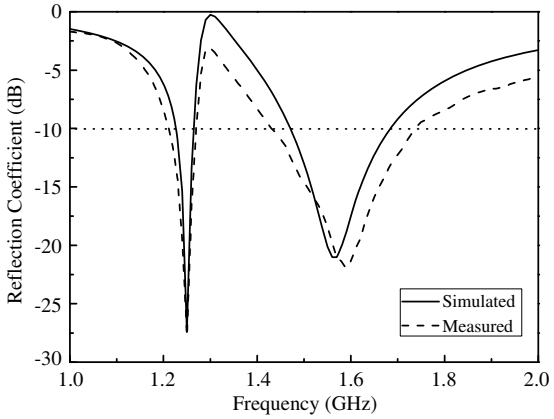

Figure 8. Simulated and measured reflection coefficient of the designed antenna.

Table 1. 6 dB beamwidth and peak gain of the designed antenna.

Frequency	Mainbeam	Measured 6 dB Beamwidth	Peak Gain	Simulated 6 dB Beamwidth	Peak Gain
1.268 GHz	Left	110° (−127° to −17°)	0.89 dBi	118° (−148° to −30°)	1.38 dBi
	Right	108° (35° to 143°)	0.65 dBi	118° (30° to 148°)	1.38 dBi
1.561 GHz	Left	113° (−128° to −15°)	1.08 dBi	120° (−149° to −29°)	1.80 dBi
	Right	107° (32° to 139°)	0.85 dBi	119° (29° to 148°)	1.80 dBi
1.575 GHz	Left	115° (−127° to −12°)	1.30 dBi	119° (−148° to −29°)	1.83 dBi
	Right	110° (31° to 141°)	1.08 dBi	119° (29° to 148°)	1.83 dBi

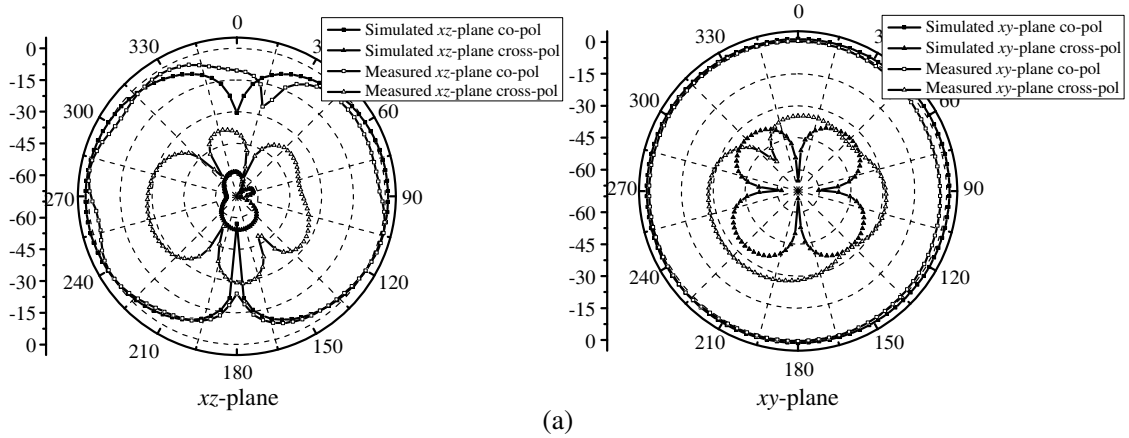

(a)

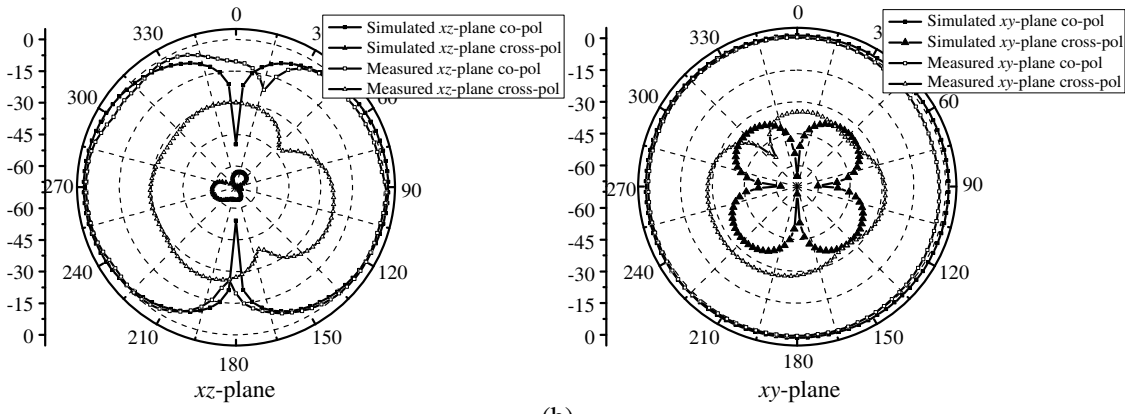

(b)

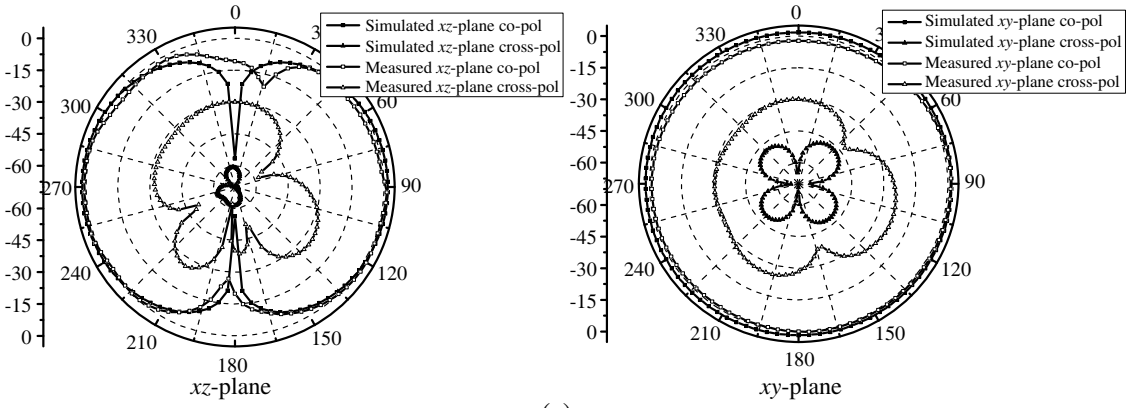

(c)

Figure 9. Measured and simulated 2-D radiation patterns at (a) 1.268 GHz, (b) 1.561 GHz, and (c) 1.575 GHz for the proposed antenna (Unit: dBi).

simulated figure, excellent omnidirectional performance is observed. The measured results show that the non-circularity in the xy-plane is less than 2 dB.

4. CONCLUSION

In this paper, a hybrid antenna by combing a conical antenna and a T-shaped monopole for multiband GNSS applications is designed. A detailed description of the operating principle of the proposed antenna in exciting the resonant modes for the desired band operation has been provided, and the antenna parameters have also been optimized. It can be found that the measured results show -10 dB impedance bandwidths of 4.7% centered at 1.268 GHz, 19.9% centered at 1.561 GHz and 19.7% centered at 1.575 GHz, respectively. Moreover, the proposed antenna has a stable radiation pattern in the xy-plane, obtaining good non-circularity characteristic less than 2 dB. And the measured 6 dB beamwidth is about 110° over the whole bandwidth in the xz-plane. The proposed antenna in this paper is promising to be a valuable candidate for GNSS signal reception on small artillery projectiles.

ACKNOWLEDGMENT

This work was supported by the National Natural Science Foundation of China under Grant No. 61172020.

REFERENCES

1. Li, J., H. Shi, H. Li, and A. Zhang, "Quad-band probe-fed stacked annular patch antenna for GNSS applications," *IEEE Antennas Wireless Propagation Letters*, Vol. 13, 372–375, 2014.
2. Bang, J.-H., B. Enkhbayar, D.-H. Min, and B.-C. Ahn, "A compact GPS antenna for artillery projectile applications," *IEEE Antennas Wireless Propagation Letters*, Vol. 10, 266–269, 2011.
3. Li, B., S.-W. Liao, and Q. Xue, "Omnidirectional circularly polarized antenna combining monopole and loop radiators," *IEEE Antennas Wireless Propagation Letters*, Vol. 12, 607–610, 2013.
4. Yu, D., S.-X. Gong, Y.-T. Wan, and W.-F. Chen, "Omnidirectional dual-band dual circularly polarized microstrip antenna using TM_{01} and TM_{02} modes," *IEEE Antennas Wireless Propagation Letters*, Vol. 13, 1104–1107, 2014.
5. Huang, H.-C., J.-C. Lu, and P. Hsu, "A compact dual-band printed Yagi-Uda antenna for GNSS and CMMB applications," *IEEE Transactions on Antennas and Propagation*, Vol. 63, No. 5, 2342–2348, 2015.

6. Li, W.-M., B. Liu, and H.-Y. Zhao, "Parallel rectangular open slots structure in multiband printed antenna design," *IEEE Antennas Wireless Propagation Letters*, Vol. 14, 1161–1164, 2015.
7. Park, B.-Y., M.-H. Jeong, and S.-O. Park, "A magneto-dielectric handset antenna for LTE/WWAN/GPS applications," *IEEE Antennas Wireless Propagation Letters*, Vol. 13, 1482–1485, 2014.
8. Jagnow, P. G. and W. C. Jennings, "Artillery fuse antenna for positioning and telemetry," US Patent No. 6020854, Feb. 1, 2000.
9. Zhang, Y.-Q., J.-W. Rong, X. Li, L. Yang and S.-X. Gong, "Novel wideband omnidirectional antenna for wireless applications," *Progress In Electromagnetics Research C*, Vol. 40, 257–267, 2013.
10. Saurav, K., D. Sarkar, and K. V. Srivastava, "CRLH unit-cell loaded multiband printed dipole antenna," *IEEE Antennas Wireless Propagation Letters*, Vol. 13, 852–855, 2014.
11. Quan, X. L., R.-L. Li, J. Y. Wang, and Y. H. Cui, "Development of a broadband horizontally polarized omnidirectional planar antenna and its array for base stations," *Progress In Electromagnetics Research*, Vol. 128, 441–456, 2012.
12. Tze-Meng, O., K. G. Tan, and A. W. Reza, "A dual-band omni-directional microstrip antenna," *Progress In Electromagnetics Research*, Vol. 106, 363–376, 2010.
13. Hsieh, W.-T. and J.-F. Kiang, "Small broadband antenna composed of dual-meander folded loop and disk-loaded monopole," *IEEE Transactions on Antennas and Propagation*, Vol. 59, No. 5, 1716–1720, 2011.
14. Ma, J., Y.-Z. Yin, S.-G. Zhou, and L.-Y. Zhao, "Design of a new wideband low-profile conical antenna," *Microwave and Optical Technology Letters*, Vol. 51, No. 11, 2620–2623, 2009.
15. Aten, D. W. and R. L. Haupt, "A wideband, low profile, shorted top hat monocone antenna," *IEEE Transactions on Antennas and Propagation*, Vol. 60, No. 10, 4485–4491, 2012.
16. Rama Rao, B., W. Kunysz, R. Fante, and K. McDonald, *GPS/GNSS Antennas*, Artech House, 2013.
17. Kraus, J. D. and R. J. Marhefka, *Antennas: For all Applications*, New York, 2002.